Magnetic artifacts due to spatial aliasing effect: a case from southeast Minas Gerais aeromagnetic dataset

Tobias Maia Rabelo Fonte-Boa, Aline Tavares Melo e Tiago Amâncio Novo

Abstract

We present a preliminary effort to solve the aliasing effect faced by aeromagnetic data processing and interpretation. The aliasing problem is caused by the survey arrangement and results in expressive magnetic artifacts after data interpolation. The spectral characteristics of the artifacts are similar to geological high-frequency magnetic features. Thus, it is very important to remove these artifacts to access the correct geophysical information. As the first approach, we applied two automated methods, the Keating and the Naprstek and Smith methods. Both methods were able to remove the undesired artifacts. They eliminate most of all the aliasing effects and enhanced the geophysical features. However, the procedures do not effectively remove all the artifacts. Therefore, further investigation applying other techniques (e.g. inverse interpolation and constrained coherence-enhancing diffusion filtering) is required to remove this effect that masks the true geological signal.

Introduction

Several researches attribute magnetic artifacts to the geophysical survey arrangement (HANSEN, 1993; YUNXUAN, 1993; KEATING, 1997; O'CONNELL *et al*., 2005; SMITH e O'CONNELL, 2005, 2007; GUO *et al*., 2012; ZHANG *et al*., 2012; GENG *et al*., 2014; NAPRSTEK e SMITH, 2016). Aspects such as sample direction and data density distribution with respect to the main geological strike are the principal causes of spatial aliasing. It results in magnetic artifacts after interpolation. These artifacts are frequently called as "boudinage pattern", "bull's-eyes", "string-of-beads" or "stepladder" in the bibliography.

In this study we present some examples of aliasing problems faced during processing and interpretation of aeromagnetic data from southeast region of Minas Gerais state in Brazil (Fig. 1). In the data set, the sample density was significantly greater in the N-S direction (one sample every 7 m) than in the W-E direction (one sample every 500 m) (LASA, 2011). As showed below, the data interpolation using the most common gridding algorithms (e.g. minimum curvature and bidirectional) resulted in spatial aliasing of the magnetic features, especially of those not perpendicular to the survey lines.

Several techniques have been put forward to solve aliasing artifacts in aeromagnetic maps (e.g. HANSEN, 1993; YUNXUAN, 1993; KEATING, 1997; O'CONNELL *et al*., 2005; SMITH e O'CONNELL, 2005, 2007; GUO et al., 2012; ZHANG *et al*., 2012; GENG *et al*., 2014; and NAPRSTEK e SMITH, 2016, 2019).

KEATING (1997) presents an algorithm that automatically joins similar magnetic features on a geodatabase, such as highs and lows, to identify magnetics trends. Based on this, extra data are added between flight lines eliminating the artifacts during the interpolation. On the other hand, NAPRSTEK e SMITH (2019) present a method which utilizes structure tensors and derivative expansions to enforce trends in the already interpolated data.

In this study, we show how the gridding artifacts overlap and mask important geological features of the study area. Then we present some preliminary results of using both methods.

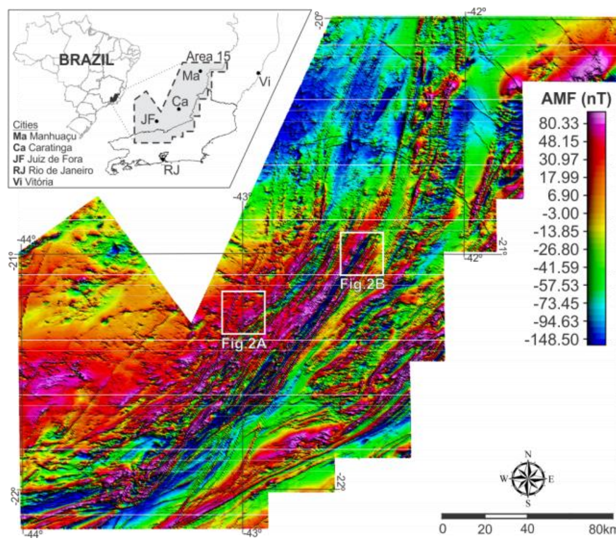

Figure 1 *– Anomalous Magnetic Field map of aerogeophysical data from Area 15 survey. The sensor height is 100 m, the line spacing is 500 m, and the grid-cell size is 100 m. Shading declination 45º.*

Magnetic artifacts on SW Minas Gerais data

In the AMF map (Fig.1) the narrow magnetic features form an acute angle with respect to flight lines, consequently, are imaged as discontinuous anomalies looking like "string of beads" or as various aligned ellipsoidal anomalies at flight line intersections. This effect can be observed in figure 2A, 2B, extracted as examples, A and B, respectively, of artifacts occurrences from the figure 1.

The two figures (Fig. 2A and 2B) show magnetic features trending in different angles with respect to the survey direction. As the angular difference between the flight lines and the magnetic features decrease the distance between the boudinage artifacts increases.

The figure 2B shows the magnetic response of a series of parallel narrow features trending NE-SW. Simultaneously, it exhibits a magnetic linear pattern trending NW-SE. This kind of feature can be observed in others regions of the map, including in figure 2A. We interpret the NW-SE pattern as an artifact caused by spatial interference due to side-by-side trend of boudinage artifacts of a group of parallel narrow magnetic features.

Therefore, there are two styles of artifacts approached in this study. There are the “beads” or boudinage artifacts represented by small ellipsoids at flight line intersection and there are the linear artifacts due to side-by-side spatial interference between the first ones.

As described in the method section, these artifacts were tested by changing the algorithm technique and setting different grid cell size values (e.g. 100m, 125m, 250m, 500m) during interpolation. Regardless the technique and the parameters, both kinds of artifacts are always evident.

To an accurate investigation, let us take the magnetic data from figure 2A as an example. It is a good situation because it displays magnetic structures trending in multiple directions (around N45ºE and N15ºE) affected by the two expressions of artifacts approached in this study.

The Radially Power Spectrum (RPS) from figure 2A is shown in the figure 3A. The slope of the spectrum indicates three distinct magnetic contributions (SPECTOR e GRANT, 1970). By applying the matched bandpass filtering (PHILLIPS, 2001) is possible to separate the magnetic anomalies produced by each of the three magnetic components (Fig. 3A).

As shown in the figure 3A the component “I”, long-wavelength values in the spectrum, symbolizes deep magnetic features trending about N15ºE to N45ºE. It is clear that are no sign of artifacts in this component.

The component “II”, intermediate wavelength values in the spectrum, represents shallow magnetic features. This component is strongly affected by aliasing and, consequently, full of artifacts (SE-NW linear pattern) as emphasize by the tilt derivative map (Fig. 3B).

The component “III” represents the magnetic signal with short-wavelength values. It seems to be aliased, but not as evident as component II due to the presence of very short-wavelength noise.

As shown previously, the artifacts seem to be more serious than just an imagery concern or a superficial issue related with noisy signal. They change the intermediate depth component of the spectrum, affecting the geophysical-geological interpretation. Due to their similar aspects, comparing with real geological high-frequency magnetic features, it is impossible to distinguish between them by a simple filtering process such as bandpass filtering. Furthermore, these features get more evident by subsequent processing such as reduction to the pole.

Hence, is very important to remove these artifacts to access the correct geophysical information given by the shallow components of the anomalous magnetic field.

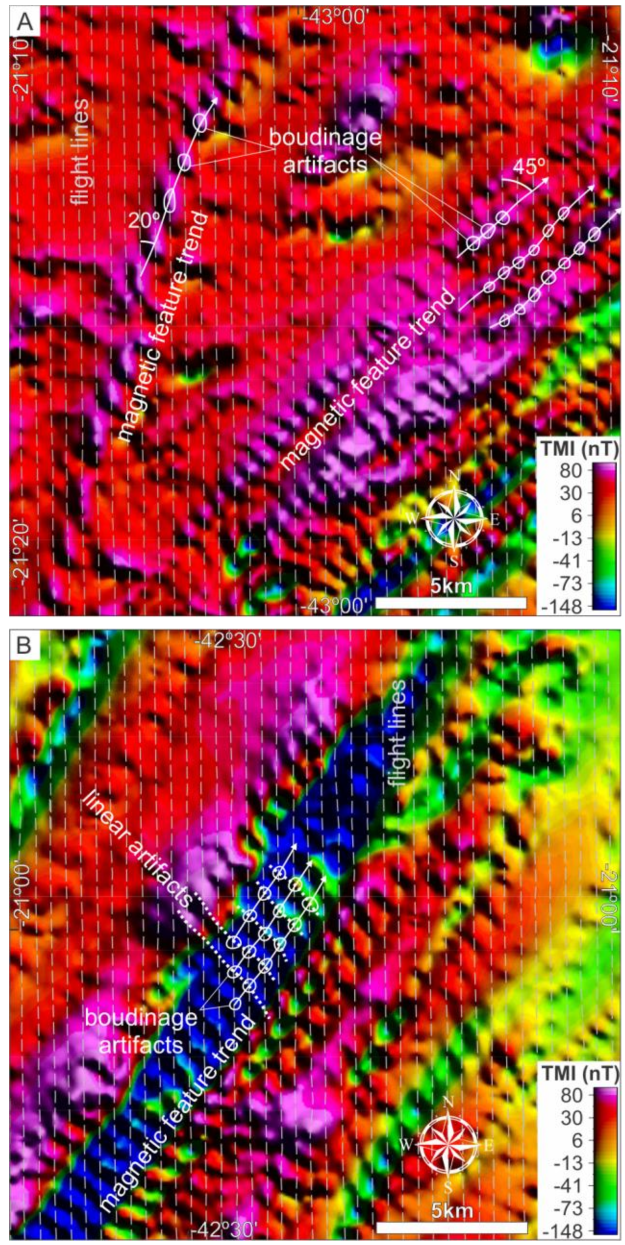

***Figure 2** – A) Example A: boudinage artifacts due to spatial aliasing of oblique-narrow magnetic features in respect to sample lines. B) Example B: linear artifacts due to side-by-side trend of boudinage artifacts of a group of parallel narrow magnetic features. Shading declination 45º.*

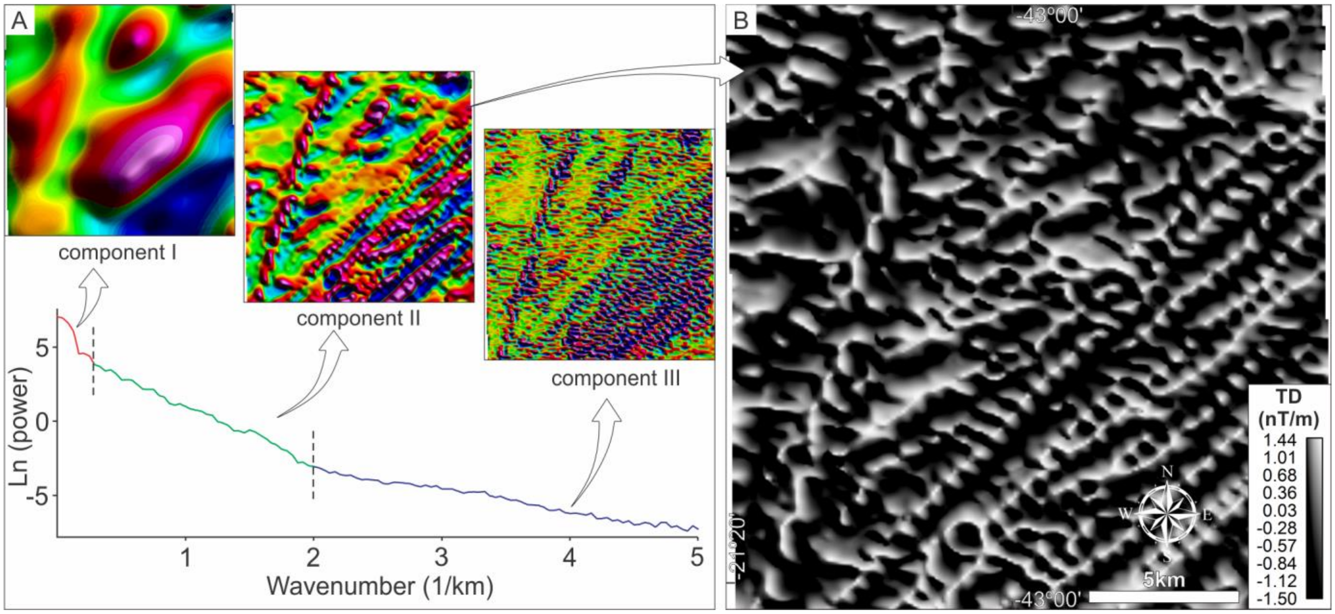

***Figure 3** – A) Radially Power Spectrum (RPS) from the example A (Fig. 2A) and the three magnetic components from matched bandpass filtering (PHILLIPS, 2001). B) Tilt derivative of the component II emphasizing the artifacts presence in the intermediate wavelength values from the RPS. Shading declination 45º.*

Methods

The Keating method

This algorithm was originally design by KEATING (1997) and was automated and available by Geosoft software. It identifies local trends in a database to enhance the magnetic trends during the gridding process, thus, solving the aliasing problem. It is executed in two steps. Firstly, the algorithm joins highs to highs and lows to lows. This step is called Find Trend Lines, and it is based on a nearest neighbor search (DAVIS, 1973) of the maxima and minima. Then, according to 8 parameters given by the user (Table 1), the maxima or minima are connected with its nearest flight-line maximum or minimum to form trend lines.

The trends are sampled as new lines in the database. Then, this new database information is used on the gridding process.

If there is more than one trending direction, the tool allows performing the Find Trend Lines process more than once with different parameters values. The multiple-direction trend information are separately appended to the database and each of them can be used or not in the gridding process.

Table 1 – Parameters used in the find trend steps.

Parameters	N45ºE	N35ºE	N15ºE
(1)Window for Max-Min Search	500	700	2000
(2)Preferred angle for trend	45	55	75
(3)Allowable deviation in angle	40	40	25
(4)Maximum length for joins	1000	1200	2500
(5)Maximum deflections for joins	-	-	-
(6)Minimum length for trend line	5000	5000	5000
(7)Resampling interval along trend	-	-	-
(8)Trend line breaking angle	-	-	-
	ex. A	ex. B	ex. A

The Naprstek and Smith method

Recently, NAPRSTEK e SMITH (2019) present a new method for interpolating linear features in aeromagnetic data which the code is available as a Geosoft executable on Naprstek Github repository. Basically, the algorithm applies a Taylor series expansion (ABRAMOWITZ e STEGUN, 1970) on the previously interpolated data and compute eigenvalue decomposition to develop a new grid with enhanced directional information (eigenvalues and eigenvectors). This information will be used to enforce linear trends across the flight lines.

Five parameters, which have significant outcomes, must be defined by the user in the process. (1) Interpolation distance, φ: represents the maximum search distance along trend direction, according to the authors it is more effective if it ranges within 50-75% of the flight line spacing; (2) Theta, θ: represents the maximum angular search variation along the trend direction; (3) Trending factor or trend strength, τ: represents the weight on the trend will be trended; (4) number of iterations: number of iterations in the interpolation loop. It has an automatic stop option; (5) subsampling: for effectiveness the process requires half of the conventional interpolation cell size. Thus, in the end of the process, the method can subsample the entire grid up to more appropriate cell size.

The parameters used for the example A were: φ = 250 m, θ = 10º, τ = 100, 300 interactions, and subsample of 50 m. For the example B: φ = 300 m, θ = 10º, τ = 100, 300 interactions. The subsample was not used for example B.

Aerogeophysical survey and interpolation parameters

The aeromagnetic data used in this study is part of a regional airborne dataset provided by the governmental institutions, CODEMGE (Companhia de Desenolvimento de Minas Gerais) and CPRM (Brazilian Geologic Survey). The survey, called Area 15, was carried out from December, 2010 to July, 2011 by Lasa Engenharia e Prospecções. The data were acquired along N-S flight lines with 500 m spacing and 100 m terrain clearance (LASA, 2011).

Total Magnetic Intensity (TMI) data were corrected for diurnal and geomagnetic field (IGRF). Firstly, the Anomalous Magnetic Field (AMF) (Fig.1) was interpolated using the bi-directional algorithm with a square mesh of 100 m cell size. Secondly, unsuccessfully trying to avoid the artifacts discussed in this study, we tested different grid cell size on the bi-directional and minimum curvature techniques as discussed in the next section.

Results

Figure 4 presents the data interpolation before (Figs. 4A and 4D) and after processing by both methods (Figs. 4B, 4C, 4E, and 4F). The results will be presented separately by each method.

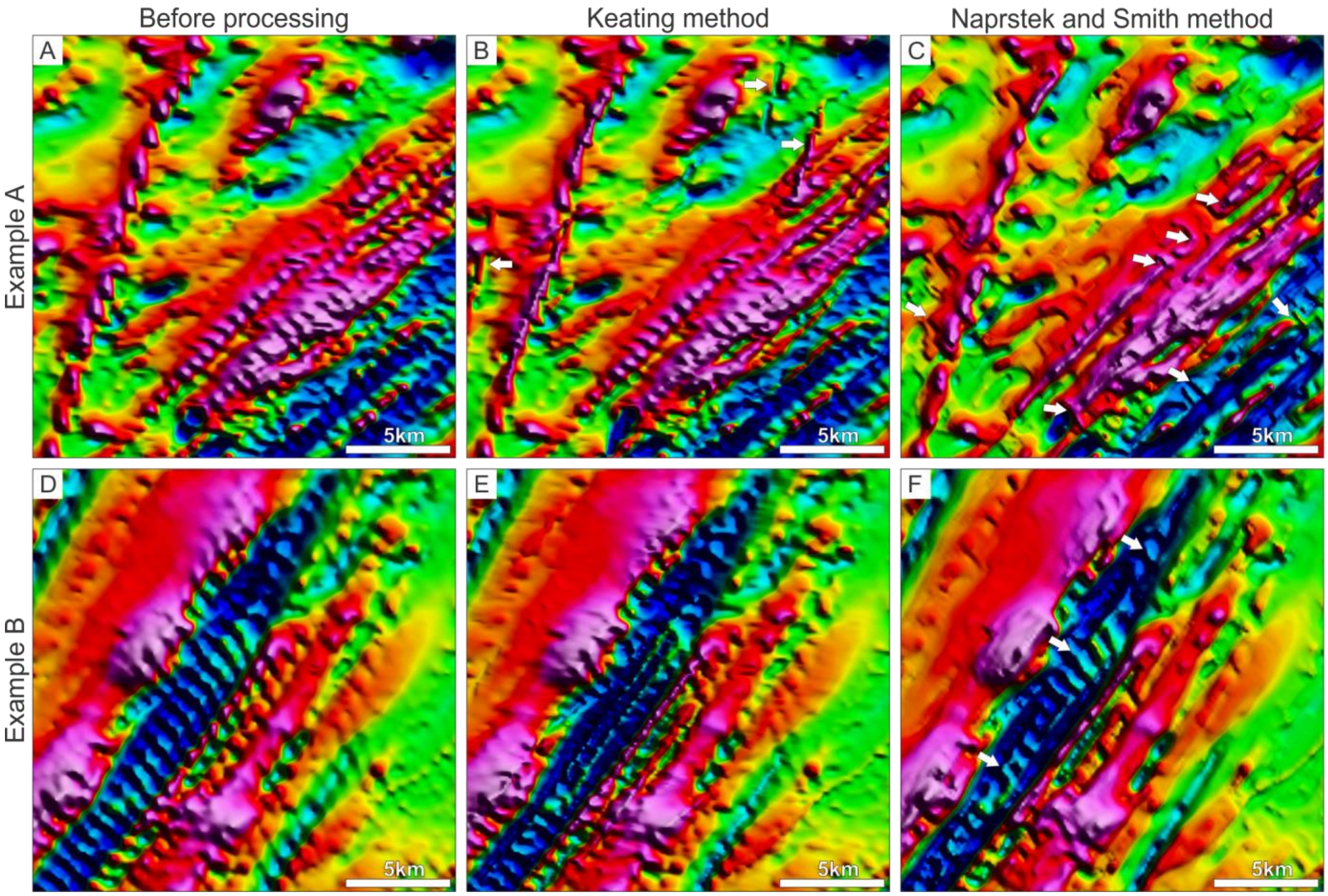

Figure 4 *– Results: A) Bi-directional interpolation of the example A at a cell size of 100m. B) Keating method interpolation of the example A using* bi-directional algorithm *at a cell size of 100 m, the processing parameters are shown in table 1; C) Naprstek method interpolation of the example A at a cell size of 100m, see the text for access the processing parameters. D) Bi-directional interpolation of the example B at a cell size of 100m. E) Keating method interpolation of the example B using* bi-directional algorithm *at a cell size of 100 m, the processing parameters are shown in table 1; F) Naprstek method interpolation of the example B at a cell size of 100m, see the text for access the processing parameters. Shading declination 45º.*

The Keating method results

The parameters used in this method are listed in table 1. The data used in the example A (Fig. 2A) has magnetic features trending approximately N45ºE, N15ºE. Thus the Finding Trend step was performed twice. On the other hand, the data used in example B (Fig. 2B) has features mainly trending N35ºE and the first step of Keating method was run once. The final grids for the example A and B are shown in figure 4B and 4E respectively.

The Keating method final grid shows substantial difference from the unprocessed grid. It was capable to enhance the most significant magnetic trends attenuating the great part of the artifacts.

The N45ºE trend, was better identified then the N15ºE and N35ºE directions. The difference in the attenuation of the artifacts is associated with the angle between the geological trend and the flight line direction. As the angular difference decreases, the distance between magnetic peaks increases requiring great values for parameters “1” and “4” (Table 1). Apparently, since these large values recognize maximum and minimum in a great distance, it could result in creating trends not related with geological features (white arrows in the figure 4B). On the other hand, the identification of features trending at an acute angle with respect to the flight lines relies on those large values parameters.

Unfortunately, the boudinage effect still fairly present the Keating method final grid (Figs. 4B and 4E), thus it partially suppressed the artifacts. It might happen because the method does not add enough spectral information about the new trended feature. Essentially, the Keating method is based in addiction of extra information on under-sampled areas over trend lines. This extra linear information appears as high-frequency sharp straight-lined anomalies connecting the beads in the final grid. Thus, due to its artificial origin, the extra data has no influence on the intermediate wavelength values of the spectrum, which is aliased and full of artifacts. Hence, this method superficially solves the artifacts problem.

The Naprstek and Smith method results

The Nasprstek and Smith method was quite effective in solving the artifact problems. It could analyze and identify the linear features and suppress most of the aliasing aspects in a multiple trend directions terrain in just one step. Visually, the method almost vanish the boudinage aspect since it generated smother linear magnetic features than the Keating method did.

However, the Naprstek method could not fully identify all the features. It can be observed in the figure 4C (white arrows) that some enhanced trends should be continuous, but are broken as interrupted features.

Locally, the method preserves the linear artifacts discussed in the previous section (indicated by white arrows in the figure 4F). It might be associated with the ratio between flight line spacing and the distance among the side-by-side parallel features. As discussed before, due to inappropriate sample spacing, nearby parallel linear features are represented as magnetic peaks closer in the flight line direction than on its own feature trend. Thus, the algorithm identifies the aside parallel feature peak as the closest maximum and ignores its own next feature maximum. It explains the local linear features trending SE-NW and the intermittent trends. Apparently, it worsens as the angular difference between the flight line and linear feature decreases. This problem is not reported in the Keating method results. It might be because it has one parameter that specifies the desirable feature angle (parameter 2, preferred angle for trends).

Conclusions

Analyzing the aeromagnetic southeast Minas Gerais data (Area 15) we conclude that its anisotropic data density and its arrangement in respect to the regional magnetic trend resulted in expressive aliasing of oblique narrow magnetic features. The interpolation of these aliasing data using the most common algorithms resulted in expressive artifacts. The artifacts are in the same spectral domain of the geological high-frequency magnetic features, making it difficult to distinguish them by filtering procedures.

As our first approach to solve this problem, we tested two methods, the Keating method and the Naprstek and Smith method. Both were capable of significantly enhance the magnetic trends and expressively solve the aliasing problem.

Unfortunately, the first one was unable to identify multiple trend directions in just one step and could not reach enough to eliminate all the aliasing spectra. The second one produced smoother linear features, apparently free of boudinage artifacts however it was ineffective in enhancing the linear features continuously.

A common problem reported in both methods was the strong dependence of the angular difference between the flight line and magnetic features. It gets difficult to identify magnetic trends as this difference decreases. The negligence in the choice of simple survey parameters such as sample direction can be irreparable and turn the data unusable. Thus, it makes clear the root dependence between the survey design and its data credibility.

Acknowledgments

We acknowledge the Companhia de Desenvolvimento de Minas Gerais (CODEMGE) and Brazilian Geologic Survey (CPRM) to provide the aeromagntic data. The first author acknowledge the Fundação de Amparo à Pesquisa do Estado de Minas Gerais (FAPEMIG) for funding the Ph.D. We also thank Dr. Richard Smith for providing code for this study.

References

ABRAMOWITZ, M. e STEGUN, I. A. Handbook of mathematical functions with Formulas, Graphs, and Mathematical Tables. Dover Publications. 1970.

DAVIS, J. C. Statistics and Data Analysis in Geology. John Wiley & Sons, Inc. 1973.

GENG, M., YANG, Q. e YUAN, Y. Trend enhancement in aeromagnetic maps using constrained coherence-enhancing diffusion filtering. Geophysics, V. 79(1), p. J1-J9, 2014.

GUO, L., MENG, X. e SHI, L. Gridding aeromagnetic data using inverse interpolation. Geophysical Journal International, V. 189, p. 1353-1360, 2012.

HANSEN, R. O. Interpretive gridding by anisotropic kriging. Geophysics, V. 58(10), p. 1491-1497, 1993.

KEATING, P. Automated trend reinforcement of aeromagnetic data. Geophysical Prospecting, V. 45, p. 521-534, 1997.

LASA. Relatório final do levantamento e processamento dos dados magnetométricos e gamaespectométricos. Levantamento aerogeofísico do estado de Minas Gerais -

Área 15 (Juiz de Fora, Cataguases, Manhuaçu). Texto técnico, 2011.

NAPRSTEK, T. e SMITH, R. A new method for aeromagnetic data interpolation with a focus on linear features. In: SEG International Exposition and 86th Annual Meeting, 2016.

NAPRSTEK, T. e SMITH, R. A new method for interpolating linear features in aeromagnetic data. Geophysics, 2019. (in press)

O'CONNELL, M. D., SMITH, R. S. e VALLÉE, M. A. Gridding aeromagnetic data using longitudinal and transverse horizontal gradients with the minimum curvature operator. The Leading Edge, V. 24, p. 142-145, 2005.

PHILLIPS, J. D. Designing matched bandpass and azimuthal filters for the separation of potential-field anomalies by source region and source type. In: 15th Geophysical Conference and Exhibition, Australian Society of Exploration Geophysicists, 2001.

SMITH, R. S. E O'CONNELL, M. D. Interpolation and gridding of aliased geophysical data using constrained anisotropic diffusion to enhance trends. Geophysics, V. 70(5), p. V121-V127, 2005.

SMITH, R. S. e O'CONNELL, M. D. An improved method for trending of features on aeromagnetic maps. In: MILKEREIT, B. ed., Proceedings of Exploration 07: Fifth Decennial International Conference on Mineral Exploration, CSEG Recorder, p. 853-861, 2007.

SPECTOR, A. E GRANT, F. Statistical models for interpreting aeromagnetic data. Geophysics, V. 35, p. 293-3302, 1970.

YUNXUAN, Z. Radon transform application to the improved gridding of airborne geophysical survey data. Geophysical Prospecting, V. 41, p. 459-494, 1993,

ZHANG, C., YAO, C. L., Xie, Y. M., ZHENG, Y. M., GUAN, H. L. e Hong, D. M. Reduction of distortion and improvement of efficiency for gridding of scattered gravity and magnetic data. Applied Geophysics, V. 9, p. 378-390, 2012.